# Measuring the Lyapunov exponent using quantum mechanics

F. M. Cucchietti,[1] C. H. Lewenkopf,[2] E. R. Mucciolo,[3] H. M. Pastawski,[1] and R. O. Vallejos[4]
[1]*Facultad de Matemática, Astronomía y Física, Universidad Nacional de Córdoba, Ciudad Universitaria, 5000 Córdoba, Argentina*
[2]*Instituto de Física, Universidade do Estado do Rio de Janeiro, 20559-900 Rio de Janeiro, Brazil*
[3]*Departamento de Física, Pontifícia Universidade Católica do Rio de Janeiro, CP 38071, 22452-970 Rio de Janeiro, Brazil*
[4]*Centro Brasileiro de Pesquisas Físicas, R. Xavier Sigaud 150, 22290-180 Rio de Janeiro, Brazil*
(Received 27 November 2001; published 1 April 2002)

We study the time evolution of two wave packets prepared at the same initial state, but evolving under slightly different Hamiltonians. For chaotic systems, we determine the circumstances that lead to an exponential decay with time of the wave packet overlap function. We show that for sufficiently weak perturbations, the exponential decay follows a Fermi golden rule, while by making the difference between the two Hamiltonians larger, the characteristic exponential decay time becomes the Lyapunov exponent of the classical system. We illustrate our theoretical findings by investigating numerically the overlap decay function of a two-dimensional dynamical system.

DOI: 10.1103/PhysRevE.65.046209 PACS number(s): 05.45.Mt, 03.65.Sq, 03.65.Yz, 73.21.−b

## I. INTRODUCTION

Over the last two decades the quest for quantum fingerprints of classical chaotic behavior has been a key subject of investigation in quantum chaos [1,2]. As a result, signatures of the classical underlying dynamics were identified in the spectra, wave functions, and time evolution of a large set of quantum systems. However, one of the simplest indications of classical chaos, namely, the Lyapunov exponent, remained unrelated to the quantum dynamics [3]. A clear advance in this direction has been made recently by Jalabert and Pastawski [4], who proposed that the classical Lyapunov exponent is measured by the decay rate of an overlap between perturbed and unperturbed quantum states evolving from the same initial state. Their work triggered several numerical studies [5–8] whose results are not always in line with the original predictions of Ref. [4]. The main goal of this paper is to discuss the range of applicability of these predictions and to understand under which conditions it is possible to extract a classical Lyapunov exponent from the quantum evolution of a system.

The object of study is the comparison between the time evolution of a wave packet under a given system Hamiltonian $H_0$ and the corresponding evolution for a different Hamiltonian $H=H_0+V$. Formally, this can be quantified by the overlap amplitude

$$O(t)=\langle\psi|\exp(iHt/\hbar)\exp(-iH_0t/\hbar)|\psi\rangle, \tag{1}$$

where for the initial state $|\psi\rangle\equiv|\psi(0)\rangle$, the Gaussian wave packet

$$\psi(\mathbf{r},t=0)=\frac{1}{(\sqrt{\pi}\sigma)^{d/2}}\exp\left[\frac{i}{\hbar}\mathbf{p}_0\cdot(\mathbf{r}-\mathbf{r}_0)-\frac{(\mathbf{r}-\mathbf{r}_0)^2}{2\sigma^2}\right] \tag{2}$$

is chosen, centered at $\mathbf{r}_0$ and with initial momentum $\mathbf{p}_0$. The purpose of such parametrization is twofold: The initial momentum $\mathbf{p}_0$ sets the wave packet mean energy range at which we define (classically) the Lyapunov exponent, whereas the choice of a Gaussian wave packet (with finite width $\sigma$) makes the theoretical considerations tractable within the semiclassical approximation.

The amplitude overlap in Eq. (1) can be interpreted in the following two different, though formally equivalent, ways.

(a) A wave packet is prepared at the time $t=0$ and allowed to evolve under $H_0$ till a time $t>0$. The resulting state is then propagated backwards in time under the Hamiltonian $H$ till $t=0$. Under such construction, $|O(t)|^2$ gives the return probability. This is the picture described by Ref. [4] that was inspired by some recent nuclear magnetic resonance experiments [9,10]. These experiments explore the scenario that, under certain circumstances, it is possible to evolve backwards in time a complex quantum system. This is in the spirit of the *gedanken* experiment at the origin of the Boltzmann-Loschmidt controversy [11] and, for that reason, we call $|O(t)|^2$ the Loschmidt echo. Due to the difference between the Hamiltonians $H$ and $H_0$, $|O(t)|^2$ is expected to decay as $t$ increases. The construction given by Eq. (1) can be regarded as a way to capture the physical effect of coupling the system to a complex time-dependent environment, and hence relate $|O(t)|^2$ to dephasing [12,13].

(b) Alternatively, one can regard $O(t)$ as the overlap amplitude of an initial state $|\psi\rangle$ propagated forward in time under $H_0$, with the same initial state $|\psi\rangle$ propagated with $H$. This interpretation is closely related to the concept of fidelity [14–16,7,8].

Let us now state the main finding of Ref. [4]. There it is was shown that, after a suitable averaging (which shall be discussed in the foregoing section), the return probability or fidelity can be separated into two contributions,

$$M(t)\equiv\overline{|O(t)|^2}=M_1(t)+M_2(t), \tag{3}$$

both described in the long-time limit as

$$M_i(t)\propto\exp(-\alpha_i t). \tag{4}$$

The decay rate $\alpha_1$ depends on the properties of the perturbation $V=H-H_0$, while $\alpha_2$ is the classical Lyapunov exponent

 

associated with the dynamics of $H_0$, provided $V$ is classically weak. Depending on $V$ and $\lambda$ the decay can be dominated by either $M_1(t)$ or $M_2(t)$. In this paper we show under which conditions it is possible to extract $\lambda$ from the analysis of the average fidelity $M(t)$.

The structure of this paper is as follows. In Sec. II we describe the model we use to obtain $\lambda$ from the quantum time evolution. Section III presents the analysis of the different decay processes that govern the fidelity $M(t)$. There we show that $M_1(t)$ is nothing else than the Fermi golden rule. The classical and quantum relevant scales to the problem are discussed. In particular, we show under which circumstances is it possible to observe the Lyapunov decay. The numerical results verifying a Lyapunov decay for our dynamical system are presented in Sec. IV. We then conclude in Sec. V by relating our findings to the recent papers mentioned above.

## II. THE MODEL

To investigate the dependence of the Loschmidt echo on the magnitude of an external perturbation, we use the smooth stadium ''billiard'' introduced in Ref. [17,18] as the unperturbed system. This model consists of a two-dimensional Hamiltonian $H_0=\mathbf{p}^2/2m+U(\mathbf{r})$ with the potential given by

$$U(\mathbf{r})=U_0\begin{cases}\infty, & x<0\\ (y/R)^{2\nu}, & 0\leqslant x<d\\ \{[(x-d)^2+y^2]/R^2\}^{\nu}, & x\geqslant d.\end{cases} \quad (5)$$

In addition, $U(\mathbf{r})=\infty$ whenever $y<0$. The exponent $\nu$ sets the slope of the confining potential. For $\nu=1$ the smooth stadium is separable and thus integrable. As the value of $\nu$ is increased, the borders become steeper. In the limit of $\nu\to\infty$, the stadium gains hard walls, becoming the well-known Bunimovich billiard, one of the paradigms of classical chaotic systems. (Actually, we consider a quarter of a stadium in order to avoid features related to parity symmetries [1]). Thus, by varying $\nu$, we can tune the system dynamics from integrable to chaotic.

In order to make the presentation more concise, throughout the paper we choose units such that $U_0=1$, $m=1/2$, and $R=d=1$. This defines units for other quantities as well, such as time. Thus, the equipotential $U(x,y)=1$ corresponds to the border of the stadium with unit radius and unit length. For any value of the energy $E$ the equipotential $U(x,y)=E$ gives the classical turning points, defining the allowed area $\mathcal{A}\equiv\mathcal{A}(E)$. This area is an important parameter in the discussion of our numerical and analytical results. Any exponent in the range $1<\nu\leqslant 2$ already leads to a mixed phase space, i.e., a situation with both regular and chaotic motions present. In particular, for $\nu\geqslant 2$, $d=1$, and total energy $E=1$ the classical dynamics is predominantly ergodic, although small remnants of integrability still exist. These observations are illustrated by the Poincaré surfaces of section displayed in Fig. 1.

The global Lyapunov exponent $\lambda$ for two-dimensional systems can be easily computed by standard methods, such as that proposed by Benettin *et al.* [19]. The evolution of the classical trajectories was carried out numerically using a symplectic algorithm [20]. We computed the Lyapunov exponent for several values of $\nu$. At $E=1$, $\lambda$ varies smoothly as a function of $\nu$, as shown in Fig. 2. As expected, as $\nu$ becomes very large, $\lambda$ approaches the value of the Lyapunov exponent for the Bunimovich stadium billiard, namely, $\lambda_{\mathrm{hard}}=0.86$.

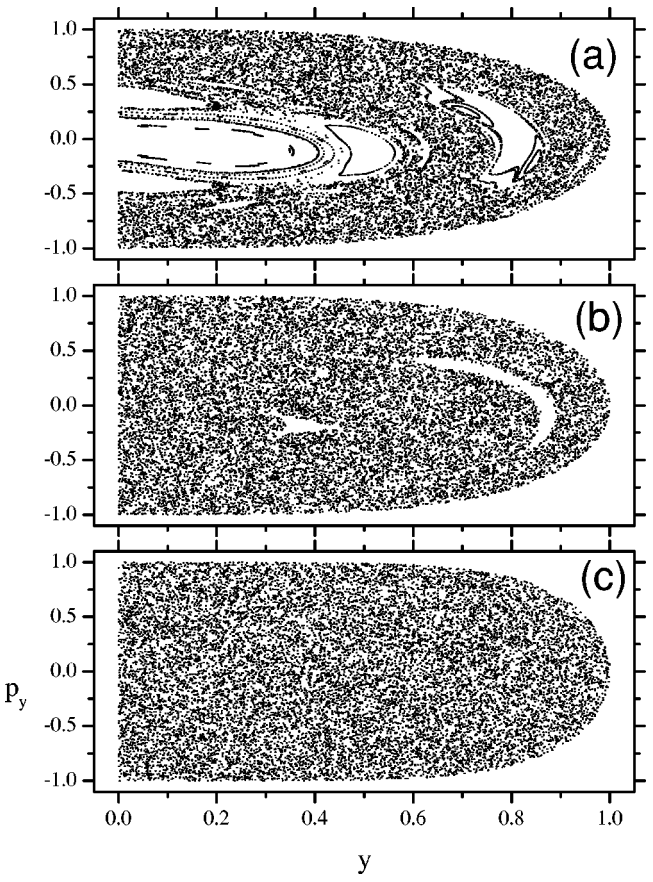


FIG. 1. Poincaré surface of section for the smooth stadium billiard for $E=1$, $R=d=1$ and (a) $\nu=1.5$, (b) $\nu=2$, and (c) $\nu=3$. (Momentum and position are measured in arbitrary units.)

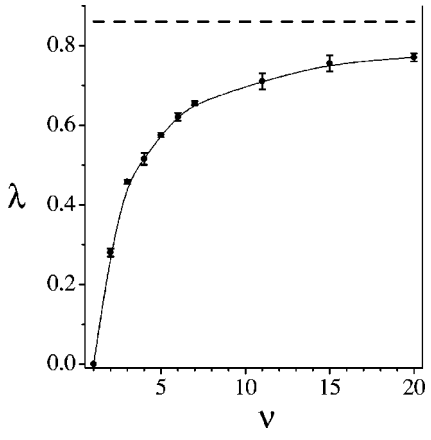


FIG. 2. Lyapunov exponent of the smooth stadium for $E=1$ as a function of $\nu$. The circles are the results of our computation, while the continuous line serves as a guide to the eye. The dashed line corresponds to the billiard limit, $\lambda_{\mathrm{hard}}=0.86$. The unit of $\lambda$ was fixed by the choice of $U_0$, $m$, $R$, and $d$.

The work of Ref. [4] used a Gaussian random background potential as the perturbation that, once suddenly switched on, mimics the effects of external sources of irreversibility in the time evolution of a real system. Thus, static disorder played the role of the external perturbation $V$. Our strategy is essentially the same: we investigate $M(t)$ numerically taking an ensemble average over different realizations of a disordered potential $V(\mathbf{r})$. For the later we choose a superposition of $\mathcal{N}_i$ independent Gaussian impurities, as in Refs. [4,21]:

$$V(\mathbf{r})=\sum_{j=1}^{\mathcal{N}_i}\frac{u_j}{2\pi\xi^2}\exp\left[-\frac{|\mathbf{r}-\mathbf{R}_j|^2}{2\xi^2}\right]. \tag{6}$$

The vector $\mathbf{R}_j$ denotes the position of the $j$th impurity. All impurities are uniformly distributed over an area $\mathcal{A}$ of the two-dimensional plane where the stadium resides, with concentration $n_i=\mathcal{N}_i/\mathcal{A}$. The strengths $u_j$ are Gaussian distributed and uncorrelated, i.e., $\overline{u_j u_{j'}}=u^2\delta_{jj'}$, with $\overline{u_j}=0$. The impurity potential defined above is statistically characterized by the correlation function

$$C(|\mathbf{r}-\mathbf{r}'|)\equiv\overline{V(\mathbf{r})V(\mathbf{r}')}=\frac{u^2 n_i}{4\pi\xi^2}\exp\left[-\frac{|\mathbf{r}-\mathbf{r}'|^2}{4\xi^2}\right] \tag{7}$$

(implicitly assuming $\xi\ll\sqrt{\mathcal{A}}$). Notice that impurity averaging yields $\overline{V(\mathbf{r})}=0$.

## III. THEORETICAL BACKGROUND

This section is devoted to the analysis of the time dependence of the fidelity $M(t)$, explaining the origin of its different decay laws. We discuss the relation between the decay regimes associated to $M(t)$ and the different time and perturbation strength scales of the system. These considerations solve the recent controversy between Lyapunov versus Fermi golden rule decay [7,8].

Let us start giving a more precise definition to $M_i(t)$ appearing in Eq. (3), namely,

$$M_1(t)\equiv|\overline{O(t)}|^2 \quad \text{and} \quad M_2(t)\equiv\overline{|O(t)|^2}-|\overline{O(t)}|^2. \tag{8}$$

As it was already shown semiclassically [4], both $M_1(t)$ and $M_2(t)$ exhibit an exponential decay in time, but different in nature. We show in the sequel that the prevailing decay law is determined by the perturbation strength, as well as the time range under consideration.

### A. The semiclassical approximation scheme

The best way to identify in $O(t)$ manifestations of the classical underlying dynamics is to use a semiclassical approximation. This is the essence of Ref. [4], which presents a complete calculation scheme for $O(t)$ in the case of a chaotic $H_0$ and a ''weak'' perturbation $V$. The starting point is the Van Vleck semiclassical propagator, casted in terms of a sum over all classical trajectories $s$ going from $\mathbf{r}'$ to $\mathbf{r}$ in the time interval $t$:

$$K^V(\mathbf{r},\mathbf{r}';t)=\sum_{s(\mathbf{r},\mathbf{r}';t)}\frac{C_s^{1/2}}{2\pi i\hbar}\exp\left[\frac{i}{\hbar}S_s^V(\mathbf{r},\mathbf{r}';t)-\frac{i\pi}{2}\mu_s\right], \tag{9}$$

where $S^V$ denotes the action given by the integral of the Lagrangian, $S_s^V(\mathbf{r},\mathbf{r}';t)=\int_0^t dt' L(V)$. The superscript $V$ stands for the perturbation potential, its absence indicates $V=0$. The Maslov index corresponding to the trajectory $s$ is given by $\mu_s$ and $C_s=|\det(\partial^2 S_s/\partial r_i'\partial r_j)|$ accounts for the conservation of classical probability in going from the initial to the final position components $i$ and $j$, respectively. To proceed analytically, it is necessary to restrict the calculations to a situation where it is possible to neglect the influence of the perturbation $V$ in the coefficients $C_s$ [22]. In general, the propagator $K^V(\mathbf{r},\mathbf{r}';t)$ describes the quantum evolution problem with great accuracy up to very long times, though shorter than the Heisenberg time [23]. Since the features we are interested in are manifest in a short time scale, the semiclassical propagator is an adequate approximation.

We use $K^V(\mathbf{r},\mathbf{r}';t)$ to propagate the wave packet $\psi(\mathbf{r}',t=0)$ given by Eq. (2) at $t=0$ up to an arbitrary time $t$. After a simple integration, one obtains

$$\psi^V(\mathbf{r},t)=\sqrt{4\pi\sigma^2}\sum_{s(\mathbf{r},\mathbf{r}_0;t)}K_s^V(\mathbf{r},\mathbf{r}_0;t)\exp\left[-\frac{\sigma^2}{2\hbar^2}(\mathbf{p}_s-\mathbf{p}_0)^2\right], \tag{10}$$

where $\mathbf{p}_s$ is defined by $\partial S/\partial\mathbf{r}'|_{\mathbf{r}'=\mathbf{r}_0}=-\mathbf{p}_s$. Equation (10) is obtained under the assumption $\xi\gg\sigma\gg k^{-1}$, constraining the initial wave packet to be spatially concentrated over a region smaller in diameter than the correlation length of the fluctuations in $V(\mathbf{r})$.

We can now calculate the overlap $O(t)$ as defined by Eq. (1) by writing an analytical semiclassical expression for $\langle\psi^V(t)|\psi(t)\rangle$. For times shorter than the Heisenberg time, this is possible through the diagonal approximation [4]. This approximation is standard [24] and neglects contributions from pairs of trajectories that are different, namely, $s\neq s'$. The resulting expression reads

$$O(t)=\frac{\sigma}{\pi\hbar^2}\int d\mathbf{r}\sum_{s(\mathbf{r},\mathbf{r}_0;t)}C_s\exp\left(\frac{i}{\hbar}\Delta S_s\right)\times\exp\left[-\frac{\sigma^2}{\hbar^2}(\overline{\mathbf{p}_s}-\mathbf{p}_0)^2\right], \tag{11}$$

where the action difference $\Delta S_s$ is just

$$\Delta S_s=-\int_0^t dt' V[\mathbf{q}_s(t')]. \tag{12}$$

Notice that phase difference accumulated along a trajectory $s$ is solely due to the perturbation potential $V$.

At this level, the fidelity $M(t)$ is trivially written by taking the modulus squared of $O(t)$, which implies in summing over pairs of trajectories $s$ and $s'$ taking into account the interference between phases, $(\Delta S_s-\Delta S_{s'})/\hbar$. It is easy to check that $V=0$ leads to $M(t)=1$, as expected [4]. The

double sum we refer to can be split in two kinds of terms: (a) the diagonal ones, when the trajectories $s$ and $s'$ remain close to each other and (b) the off-diagonal terms, corresponding to an unrelated pair of trajectories $s$ and $s'$. In Ref. [4] it was shown that after disorder averaging the *diagonal* contribution renders

$$M_2(t) \propto \frac{1}{t}\exp(-\lambda t), \tag{13}$$

where $\lambda$ is the classical Lyapunov coefficient. In the long-time limit $t \gg 1/\lambda$, the exponential decay dominates and $M_2(t)$ reduces to Eq. (4). It is not within our scope to give details of this derivation, but it is worth mentioning that, after impurity averaging [21,25], the calculations leading to Eq. (13) rely solely on generic assumptions about the classical dynamics of $H_0$.

The contribution to the fidelity coming from off-diagonal terms $M_1(t)$, can be computed using the impurity average technique of Refs. [21,25]. It amounts to computing the variance of the phase appearing in Eq. (11). Assuming that $\Delta S_s$ are Gaussian distributed, which is reasonable for trajectories longer than $\xi$, one readily writes

$$\overline{\exp\left(\frac{i}{\hbar}\Delta S_s\right)} = \exp\left(-\frac{1}{2\hbar^2}\overline{\Delta S_s^2}\right), \tag{14}$$

where, by recalling Eq. (12), the impurity average $\overline{\Delta S_s^2}$ is written as

$$\overline{\Delta S_s^2} = \int_0^t dt' \int_0^t dt'' C[r(t',t'')]. \tag{15}$$

The distance in the impurity autocorrelation function $C$ is $r(t',t'') = |\mathbf{q}_s(t') - \mathbf{q}_s(t'')|$. It is useful to change integration variables to the center of mass $(q+q')/2$ and difference $q-q'$ coordinates, with $q = v_0 t$ and $q' = v_0 t'$. For $\xi \ll \sqrt{\mathcal{A}}$, it is a good approximation to extend the integral over the coordinate difference to infinity. We can make further analytical progress if we specialize the discussion to hard-wall billiard systems, which are good approximations to our model Hamiltonian, particularly as $\nu$ is increased. In this case, the integral over $(q+q')/2$ yields $L = v_0 t$. As a result, one obtains [4]

$$M_1^{\mathrm{sc}}(t) \propto \exp(-\alpha_1 t) \quad \text{with} \quad \alpha_1 = \frac{u^2 n_i}{2\sqrt{\pi}\hbar^2 v_0 \xi}. \tag{16}$$

Notice that the Gaussian ansatz for $\Delta S_s$ is not justified for very short times in the range of $\xi/v_0$, which in our case is of the same order as $\tau \equiv \sqrt{\mathcal{A}}/v_0$. Thus, we are unable to make predictions about $M_1(t<\tau)$ and, consequently, about the constant factor multiplying $\exp(-\alpha_1 t)$ in Eq. (16). The exponential decay can also be characterized by the typical length at which the quantum phase is not modified by the presence of impurities,

$$l = \frac{2\sqrt{\pi}\hbar^2 v_0^2 \xi}{u^2 n_i} = \frac{v_0}{\alpha_1}. \tag{17}$$

This quantity is known as the elastic mean free path. Equation (17) corrects a minor mistake in $l$ given by Refs. [25,4], namely, a missing factor of 1/2 [26]. In the sequel, we show the relation between this semiclassical result and the stochastic theory.

### B. The random-matrix approach

The computation of $M_1(t)$ by the statistical approach is a standard random-matrix result (see, for instance, Ref. [27] or Appendix B of Ref. [28]). A somewhat similar calculation was also recently carried out by Mello and collaborators [29]. Notwithstanding, it is instructive to describe how this is done. The connection to the random-matrix theory is made by the Bohigas' conjecture [30] and the fact that the classical dynamics of $H_0$ is chaotic. Consequently, the matrix elements

$$V_{nn'} = \langle n | V(\mathbf{r}) | n' \rangle \tag{18}$$

with respect to the eigenstates of $H_0$ are Gaussian distributed, regardless the form of $V(\mathbf{r})$. With this in mind, we can calculate the averaged propagator

$$K(t) = e^{-iHt/\hbar}\theta(t). \tag{19}$$

This task is usually carried out in the energy representation by introducing the Green function operator

$$G(E) = \frac{1}{E + i\eta - H} \quad \text{with} \quad \eta \to 0^+. \tag{20}$$

The formal expansion of $G$ in powers of $V$ and the rules for averaging over products of Gaussian distributed matrix elements give

$$\overline{G} = G_0 \frac{1}{1 - \overline{VG_0VG_0}}, \tag{21}$$

where $G_0 = (E + i\eta - H_0)^{-1}$. The matrix representation of $\overline{G}$ is particularly simple. In the eigenbasis of $H_0$, it becomes

$$\overline{G}_{nn'}(E) = \frac{\delta_{nn'}}{E + i\eta - E_n - \Sigma_n(E)}, \tag{22}$$

where $E_n$ is the $n$th eigenvalue of $H_0$ and

$$\Sigma_n(E) = \sum_{n'} \overline{V_{nn'}^2}(G_0)_{n'} \equiv \Delta_n(E) - \frac{i}{2}\Gamma_n(E), \tag{23}$$

with

$$\Delta_n(E) = \mathrm{P}\sum_n \frac{\overline{V_{nn'}^2}}{E - E_n},$$

$$\Gamma_n(E)=2\pi\sum_n \overline{V_{nn'}^2}\,\delta(E-E_n). \tag{24}$$

Here P stands for principal value. The real part $\Delta_n(E)$ only causes a small shift to the eigenenergy $E_n$ and will thus be neglected. Whenever the average matrix elements $\overline{V_{nn'}^2}$ show a smooth dependence on the indices $n$, it is customary to replace $\Gamma_n$ by its average value,

$$\Gamma=2\pi\overline{V^2}/\Delta, \tag{25}$$

where $\Delta$ is the mean level spacing of the unperturbed spectrum. In most practical cases, $\Gamma$ and $\Delta$ can be viewed as local energy averaged quantities. Hence, the average propagator in the time representation becomes

$$\overline{K}_{nn'}(t)=\delta_{nn'}\exp\left(-i\frac{E_n t}{\hbar}-\frac{\Gamma t}{2\hbar}\right)\theta(t). \tag{26}$$

It worth stressing that $\Gamma$ arises from a nonperturbative scheme; nonetheless, it is usually associated to the Fermi golden rule due to its structure.

The average propagator obtained in Eq. (26) is easily related to $M_1(t)$ by calculating $\langle\psi|\overline{K}|\psi\rangle$. This step gives us also a more precise meaning to the smooth energy dependence of $\Gamma(E)$: In our construction the latter has to change little in the energy window corresponding to the energy uncertainty of $\psi(\mathbf{r},t)$, which is determined by $\sigma$. Thus, the (random-matrix theory) RMT final expression for $M_1(t)$ is

$$M_1^{\mathrm{RMT}}(t)=\exp(-\Gamma t/\hbar), \tag{27}$$

with $\Gamma$ given by Eq. (25). Equation (27) does not hold for very short times, since we neglected the smooth energy variations of $\Gamma_n$ and $\Delta_n$. It is beyond the scope of RMT to remedy this situation, since for that purpose nonuniversal features of the model have to be accounted for.

Despite sharing the same formal structure, it remains to be shown that both semiclassical and random model theory are strictly equivalent. This is what we do next by deriving an expression for the Fermi golden rule in terms of the classical quantities used in Eq. (16).

For chaotic systems, we can calculate the average off-diagonal perturbation matrix elements using the universal autocorrelation function of eigenstates first conjectured by Berry [31]. For two-dimensional billiards this function reads

$$\langle\psi_n(\mathbf{r}_1)\psi_n(\mathbf{r}_2)\rangle=\frac{1}{\mathcal{A}}J_0(k_n|\mathbf{r}_1-\mathbf{r}_2|), \tag{28}$$

where $J_0(x)$ is the Bessel function of zero order, $k_n$ is the wave number associated to the $n$th eigenstate of $H_0$, and $\mathcal{A}$ is the billiard area. Here $\langle\cdots\rangle$ can be regarded as the average $\psi_n(\mathbf{r}_1)\psi_n(\mathbf{r}_2)$ obtained by sweeping $\mathbf{R}=(\mathbf{r}_2+\mathbf{r}_1)/2$ over a region containing several de Broglie wave lengths. Equivalently, one could also average over a large number of levels, provided that $k_n$ does not change much on that interval. For a rigorous discussion on the validity of Eq. (28) and the different averaging procedures, see Ref. [32].

Recalling Eq. (18), we can write the off-diagonal squared matrix elements averaged over the impurity realizations as

$$\overline{V_{nn'}^2}=\int d^2r_1\int d^2r_2\psi_n(\mathbf{r}_1)\psi_n(\mathbf{r}_2)\psi_{n'}\times(\mathbf{r}_1)\psi_{n'}(\mathbf{r}_2)\overline{V(\mathbf{r}_1)V(\mathbf{r}_2)}. \tag{29}$$

By changing variables to $\mathbf{R}=(\mathbf{r}_2+\mathbf{r}_1)/2$ and $\mathbf{r}=\mathbf{r}_2-\mathbf{r}_1$ and with the help of Berry's conjecture, it is straightforward to reduce the integral in Eq. (29) to

$$\overline{V_{nn'}^2}=\frac{1}{\mathcal{A}}\int d^2rJ_0(k_nr)J_0(k_{n'}r)C(r). \tag{30}$$

The correlation function $C$ is given by Eq. (7). For a sufficiently large billiard, $\xi\ll\mathcal{A}^{1/2}$, we obtain [33]

$$\overline{V_{nn'}^2}\approx\frac{n_iu^2}{\mathcal{A}}\exp[-(k_n^2+k_{n'}^2)\xi^2]I_0(2k_nk_{n'}\xi^2), \tag{31}$$

where $I_0(x)$ is the modified Bessel function of the first kind. For high-energy eigenstates, such that $k_n\xi\gg1$, and for states within an energy window corresponding to $\sigma$ $(k_n\approx k_{n'})$, the above expression is further simplified to

$$\overline{V_{nn'}^2}\approx\frac{n_iu^2}{\mathcal{A}}\frac{1}{2\sqrt{\pi}k_n\xi}. \tag{32}$$

We can now insert $\overline{V_{nn'}^2}$ into the left-hand side of Eq. (25). Recalling that the mean level spacing for a two-dimensional billiard is $\Delta=2\pi\hbar^2/(\mathcal{A}m)$ and using $\hbar k=mv_0$, we obtain

$$\frac{\Gamma}{\hbar}=\frac{u^2n_i}{2\sqrt{\pi}\hbar^2v_0\xi}. \tag{33}$$

This is exactly the same decay rate of Eq. (16). It also agrees with the quantum diagrammatic perturbation theory for the bulk in the disordered model [25].

### C. Fermi golden rule and Lyapunov decay

By employing the semiclassical approach we were able to address in detail two very distinct regimes of $M(t)$. Such approximation is the most appropriate tool to study $M(t)$ provided two conditions are met: $V$ is (a) classically weak, in the sense that classical perturbation theory applies and (b) quantum mechanically strong, meaning that one can treat the actions in Eq. (14) as Gaussian variables. In such cases, for $t\gg\lambda^{-1}$, it was found that: (a) $\ln M_2(t)\propto-\lambda t$, independently of the strength of the perturbation and (b) $\ln M_1(t)\propto-\Gamma t$, where $\Gamma\propto u^2$. As one varies the perturbation strength $u$, $M(t)$ is dominated by the smallest of $\lambda$ and $\Gamma$. In other words, within the semiclassical regime, for small values of $u$ the Fermi golden rule applies. The dependence of $M(t)$ crosses over to $\ln M(t)\propto-\lambda t$, when $\Gamma>\lambda$. Equations (13) and (16) predict for which value of $u$ this transition occurs.

It remains to be discussed what happens to $M(t)$ when $u$ does not meet neither (a) nor (b), namely, either $u$ is below

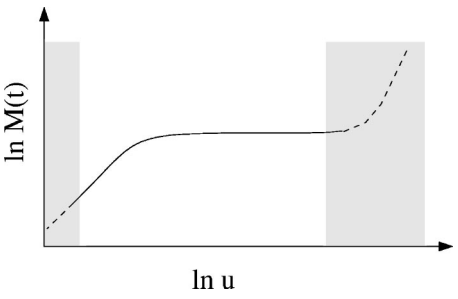


FIG. 3. Sketch of the expected behavior for $\ln M(t)$ as a function of the perturbation strength $u$ for a fixed value of $t$. The shaded fields indicate the regimes of $u$ where the semiclassical approach fails.

the Fermi golden rule regime or $u$ is in the very opposite limit of strong perturbations, above the Lyapunov regime.

Let us first discuss the limit of ''extremely'' weak perturbations, where $V$ neither significantly mixes the states of $H_0$, nor causes level crossings [34,35]. Here, $M(t)$ can be obtained by standard quantum perturbation theory. This limit was studied a long time ago by Peres [14], who found a Gaussian decay, namely, $\ln M(t) \propto -(ut)^2$. It turns out, as illustrated by our numerical study, that this limit is very hard to observe, since for very short times $M(t)$ decays as $t^2$ in all cases.

At the opposite end there is the case of ''strong'' perturbations, for which classical perturbation theory breaks down. As $u$ is augmented the Lyapunov exponents of $H_0$ and $H$ become increasingly different. Lacking a theoretical understanding for this regime, we can only speculate that $M(t)$ decays faster than in the Lyapunov regime. Here $M(t)$ will strongly depend on the specific details of $V(\mathbf{r})$.

Figure 3 summarizes the principal predictions of this section. The main feature of this diagram is the plateau in $-\ln M(t)$ vs $u$, characterizing the Lyapunov regime. For a given specific system we can predict where the plateau starts at low values of $u$. To use a quantum system to measure the Lyapunov exponent, it is crucial to know where it ends, and classical perturbation theory breaks down. For that purpose, numerical simulations were performed for the smooth stadium by varying its classical Lyapunov exponent $\lambda$ and the perturbation strength $u$. The results are presented in the following section.

## IV. NUMERICAL RESULTS

In this section we present a numerical study of $M(t)$ for the smooth stadium model with Gaussian impurity disorder introduced in Sec. II. Before showing the results, however, we describe some technical details about the numerical method employed in the simulations.

The quantum evolution of wave packets, as defined by Eq. (2), was carried out through the fourth-order Trotter-Suzuki algorithm [36]. It is worth noticing that a more straightforward approach, based on a matrix representation of the evolution operator in terms of the eigenvectors of $H_0$ would be far less efficient.

The method does not require spatial discretization of the system. However, the basis has to be such that the Hamiltonian matrix elements needs to involve only short term interactions. We thus found it useful to work on a lattice and to represent the kinetic energy with a nearest-neighbor hopping term. Within the energy range we explored, we found that a two-dimensional lattice of area $2.1R \times 1.1R$ provided very accurate results when we employed $N=180$ sites per unit distance $R$ (with the intersite distance given by $a=R/N$), corresponding to a total number of $378 \times 198$ lattice sites.

The range of parameter values explored in our simulations was limited by computational cost. Moreover, our choice of parameters was guided by the constraints imposed by the semiclassical calculations of Sec. III A. First, in order to include a large number of randomly located impurities, their correlation width $\xi$ had to be taken much smaller than $R$. Second, the semiclassical regime where Eq. (4) applies requires $\xi$ to be larger than the wave packet width $\sigma$, which, in turn, has to be much larger than the particle wavelength $\lambda_F$. Other constraints arise from finite-size effects. For instance, the large-time saturation value of the Loschmidt echo $M(t \to \infty)$ depends on the ratio $\sigma/N$. Thus, for a fixed $N$, it is necessary to make $\sigma$ as small as possible in order to guarantee a small value for $M(t \to \infty)$. In addition, let us recall that the energy spectrum of the (open boundaries) discretized system is given by

$$E_{\mathbf{k}} = \frac{2\hbar^2}{ma^2} - \frac{\hbar^2}{ma^2}[\cos(k_x a) + \cos(k_y a)]. \tag{34}$$

Therefore, we can only accurately recover the dispersion relation of the free particle, $E_{\mathbf{k}} = \hbar^2 k^2/2m$, when $ka \ll 1$. All these constraints are summarized by the inequalities

$$a \ll \lambda_F \ll \sigma < \xi \ll R. \tag{35}$$

The compromise between good accuracy and a feasible simulation time led us to set $\xi = 0.25R$, $\sigma = 0.18R$, $\lambda_F = 0.07R$, and $N=180$. This choice, combined with the values of the classical model parameters $m=1/2$ and $E=1$, gave rise to units such that $\hbar = 0.011R$. Thus, the inequalities of Eq. (35) were approximately observed in our simulations. For the quantum evolution, a time step $\delta t = 2ma^2/10\hbar = 2.8 \times 10^{-4} E/\hbar$ proved to be sufficiently small.

It is important to make a few remarks about the averaging procedure. In the simulations, besides averaging over impurity configurations, we also found important to average over initial positions $\mathbf{r}_0$ and directions $\mathbf{p}_0$. The main reason is that numerical simulations of billiards deal with relatively small, confined systems and directionality has a strong influence in the short-time dynamics.

The initial conditions for the quantum evolution were chosen from a subset that also minimized finite-size effects. That is, we chose initial conditions that allowed for the observation of an exponential decay before the saturation time. For that purpose, we took $0.5R < x_0 < R$, $0.2R < y_0 < 0.5R$, and initial momentum $\mathbf{p}_0$ such that the first collision with the boundary occurred at $x > R$, avoiding trajectories close to bouncing ball-like modes along $y$. (Such trajectories were

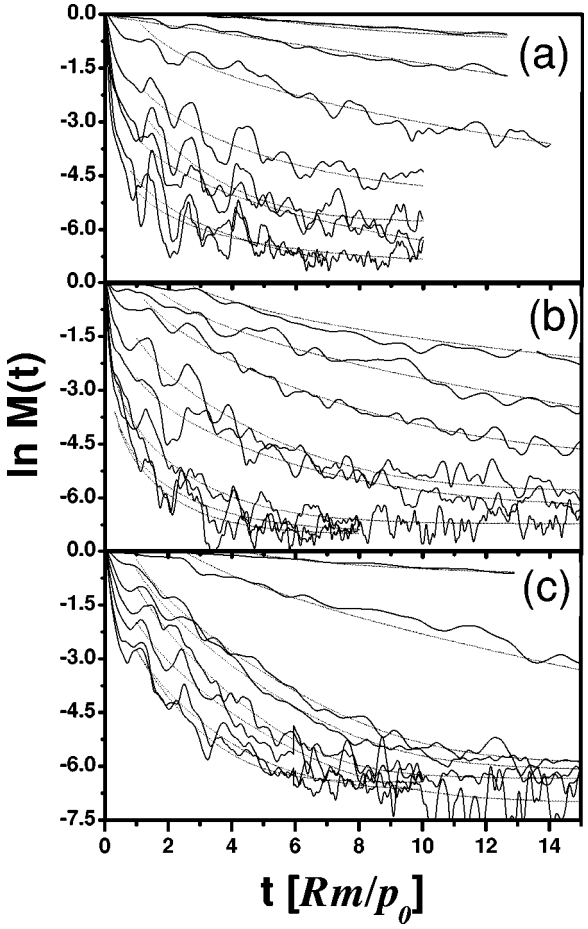


FIG. 4. $M(t)$ for $\nu=1.5$ (a), 2 (b), and 3 (c) for different values of the perturbation strength: $u=0.002$, 0.005, 0.01, 0.02, 0.03, 0.04, 0.05, and 0.06 (the units of $u$ are fixed by the choice of $U_0$, $m$, $R$, and $d$).

found to lead to strong nonexponential decays in $M(t)$ for time intervals shorter than the saturation time.)

In Fig. 4 we show $M(t)$ for $\nu=1.5$, 2, and 3 for different values of the perturbation strength. In all graphs we see that the asymptotic decays are approximately exponential within a certain ranges of $u$, as predicted in Ref. [4]. In order to obtain the characteristic decay times, we fitted $\ln M(t)$ to the function $\ln[A\exp(-t/\tau_\phi)/t+M_\infty]$. The fit was performed for times $t>R/v$, where $v=\sqrt{2E/m}=2$ is the wave packet velocity, to exclude the initial, nonuniversal (and nonexponential) time evolution. It is worth noticing that the usual nonlinear fitting procedures are rather insensitive to certain combinations of parameters $\tau_\phi$ and $A$. Thus, while the parameter $M_\infty$ could be fixed by averaging the long-time tail of the data, we avoided the uncertainty in $A$ and $\tau_\phi$ by fixing the value of the fitted curve at the initial point to be exactly equal to the respective data value. We checked that such procedure yield values for $A$ that are proportional to $u^{-2}$, as expected.

The typical number of samples used in the averaging procedure [for each trace of the $M(t)$ shown] was in the range 80–100. In fact, we observed that the number of samples needed to obtain comparable statistical mean squares fluctuation for $M(t)$ scaled with the perturbation strength $u$. That is, the larger the perturbation, the larger the fluctuations in $M(t)$ were. This fact sets another practical limit to the range of perturbation strengths $u$, we could investigate in our numerical simulations.

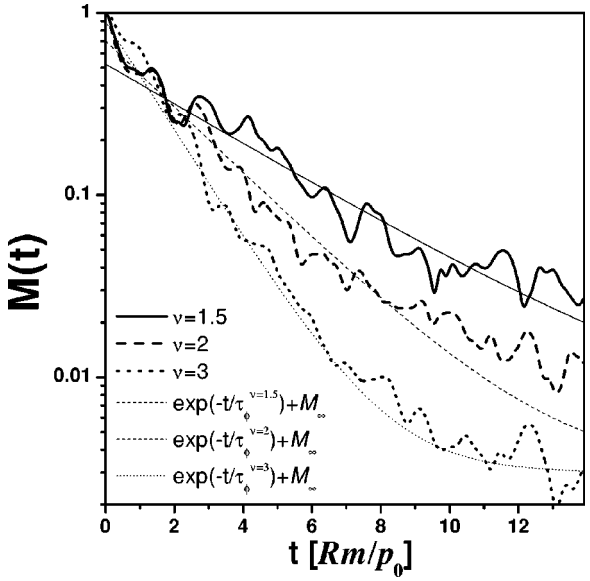


FIG. 5. Fidelity as a function of time. $u=0.01$ for $\nu=1.5$, 2, and 3. The number of samples used in the averaging behind the $\nu=1.5$ curve was 80. 100 samples were used in the two other cases.

In Fig. 5, we show the fidelity curves for the same perturbation strength, but different steepness of the confining potential. Notice that the fluctuations around the (exponential) fitted curve increase as the billiard walls become softer.

In Fig. 6, we have plotted the inverse characteristic decay times $1/\tau_\phi$ obtained in the fittings as a function of the impurity strengths $u$ for the three values of $\nu$. For comparison, we

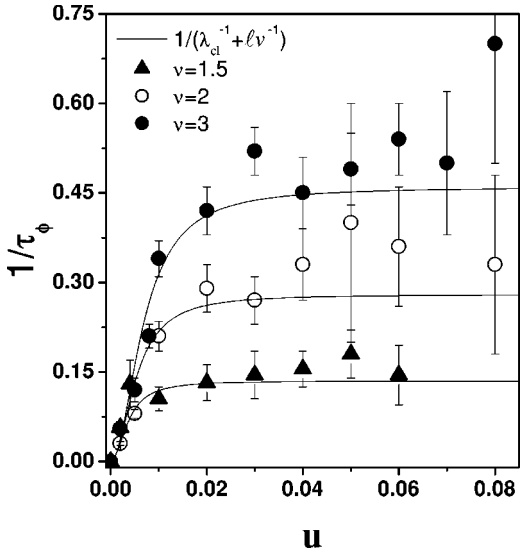


FIG. 6. Characteristic decay rates obtained from Fig. 4 as a function of perturbation strength. The solid curves correspond to the phenomenological expression (36). The units of $1/\tau_\phi$ and $u$ were fixed by the choice of $U_0$, $m$, $R$, and $d$.

plotted the phenomenological curve

$$\tau_{\text{phenom}}(u)=\frac{1}{\lambda}+\frac{1}{\alpha_1(u)}, \tag{36}$$

where $\lambda$ is the classical Lyapunov ($u$ independent) and $\alpha_1 = v_0/l$ is the characteristic decay rate obtained in Sec. III A. Such curve matches the expected asymptotic behaviors for $1/\tau_\phi$ at small and large values of $u$.

The most pronounced feature shared by all data sets is the existence of a plateau around the classical Lyapunov exponent $\lambda$, as expected. The semiclassical theory [4] predicts that this saturation should appear when the perturbation is quantum mechanically strong, but classically weak. This condition, already presented in Eq. (35), can be translated into the inequality $\lambda \ll v/l$. Indeed, the results of the simulations, as presented in Fig. 6, are consistent with the existence of a plateau in $1/\tau_\phi$ for $u$ within this range. For weak perturbations, the data is also consistent with the quadratic behavior of $\alpha_1$.

## V. CONCLUSIONS

We studied the time evolution of two wave packets prepared at the same initial state and time, but evolving under slightly different Hamiltonians, namely, $H_0$ and $H=H_0+V$. For those systems for which the Hamiltonian $H_0$ is classically chaotic, the wave packet overlap decays exponentially in time, according to the semiclassical theory [4]. For the model Hamiltonian introduced in Sec. II, we numerically verified that the exponential decay is indeed observed for a broad range of typical strengths of $V$.

Within the regime of perturbations that are quantum mechanically strong, but classically weak, the semiclassical theory predicts two decay laws [4]. While the first one is governed by the mean free path and the wave packet mean velocity $\alpha_1 = v_0/l$, the second decay law is characterized by the Lyapunov exponent, namely $\alpha_2=\lambda(E)$. By estimating the variance of $V_{nn'}$, we showed that $\alpha_1$ is nothing else than the Fermi golden rule of Ref. [7]. Our analytical findings are in quantitative agreement with the numerical results obtained from the smooth stadium.

Finally, for sufficiently long times we were able to qualitatively understand the behavior of the fidelity $M(t)$ as a function of the strength $u$ of $V$. For very weak $u$, quantum perturbation theory applies and $\ln M(t) \propto -(ut)^2$ [14]. Increasing $u$, one enters in a regime where although quantum perturbation theory breaks down, the classical one still holds. We call this the semiclassical regime. Here, we quantified the crossover from the Fermi golden rule decay to the Lyapunov decay. Finally, by further increasing $u$, classical perturbation is no longer valid and the semiclassical approximation ceases to be useful. This picture is illustrated by Fig. 3 and nicely numerically verified by Fig. 6. The plateaus obtained in the simulations show that it is possible to measure the classical Lyapunov exponent with quantum mechanics over a broad range of perturbation strengths.

Recently, Benenti and Casati [37] investigated the function $M(t)$ for a different dynamical system. Their numerical analysis gives results similar to ours, thus providing further support to our conclusions.

## ACKNOWLEDGMENTS

We thank L. Kaplan, T. H. Seligman, and F. Toscano for useful discussions at the Centro Internacional de Ciências (Mexico). This work was partially supported by a grant from Fundação VITAE. C.H.L., E.R.M., and R.O.V thank the Brazilian funding agencies CNPq, FAPERJ, and PRONEX for financial support. H.M.P. is affiliated to CONICET and F.M.C. is supported by SeCyT-UNC.

[1] F. Haake, *Quantum Signatures of Chaos* (Springer, Berlin, 2000).
[2] H.-J. Stöckmann, *Quantum Chaos: An Introduction* (Cambridge University Press, Cambridge, UK, 1999).
[3] However, the eigenvalues of the monodromy matrix can be measured by wave packets launched at the vicinity of periodic orbits, like in E. J. Heller, in *Chaos and Quantum Physics*, edited by M. J. Giannoni, A. Voros, and J. Zinn-Justin (Elsevier Science Publishers, North-Holland, Amsterdam, 1991), p. 547.
[4] R. A. Jalabert and H. M. Pastawski, Phys. Rev. Lett. **86**, 2490 (2001).
[5] F. M. Cucchietti, H. M. Pastawski, and D. A. Wisniacki, e-print cond-mat/0102135.
[6] T. Prozen, e-print quant-ph/0106149.
[7] Ph. Jacquod, P. G. Silvestrov, and C. W. J. Beenakker, Phys. Rev. E **64**, 055203 (2001).
[8] N. R. Cerruti and S. Tomsovic, e-print nlin.CD/0108016.
[9] H. M. Pastawski, P. R. Levstein, and G. Usaj, Phys. Rev. Lett. **75**, 4310 (1995).
[10] G. Usaj, H. M. Pastawski, and P. R. Levstein, Mol. Phys. **95**, 1229 (1998).
[11] R. Balian, *From Microphysics to Macrophysics* (Springer, New York, 1991), Vol. I.
[12] Y. Imry, *Introduction to Mesoscopic Physics* (Oxford, New York, 1997).
[13] Z. P. Karkuszewski, C. Jarzynski, and W. H. Zurek, e-print quant-ph/0111002.
[14] A. Peres, Phys. Rev. A **30**, 1610 (1984).
[15] S. A. Gardiner, J. I. Cirac, and P. Zoller, Phys. Rev. Lett. **79**, 4790 (1997); *ibid.* **80**, 2968(E) (1998).
[16] A. Peres, *Quantum Theory: Concepts and Methods* (Kluwer, Dordrecht, The Netherlands, 1993).
[17] R. O. Vallejos, C. H. Lewenkopf, and E. R. Mucciolo, Phys. Rev. B **60**, 13 682 (1999).
[18] J. S. E. Ortiz and A. M. Ozorio de Almeida, Physica D **145**, 293 (2000).
[19] G. Benettin, L. Galgani, and J.-M. Strelcyn, Phys. Rev. A **14**, 2338 (1976).
[20] H. Yoshida, Phys. Lett. A **150**, 262 (1990).

[21] K. Richter, D. Ullmo, and R. A. Jalabert, Phys. Rev. B **54**, R5219 (1996).
[22] This is a standard approximation in the semiclassical approach. It will be accurate up to times of the order of the inverse Lyapunov exponent. Our numerical simulations show that it still works for larger times scales.
[23] S. Tomsovic and E. J. Heller, Phys. Rev. Lett. **67**, 664 (1991).
[24] A. M. Ozorio de Almeida, C. H. Lewenkopf, and E. R. Mucciolo, Phys. Rev. E **58**, 5693 (1998).
[25] K. Richter, D. Ullmo, and R. A. Jalabert, J. Math. Phys. **37**, 5087 (1996).
[26] In Ref. [25], the result of integral in Eq. (3.12), taken from $-\infty$ to $\infty$, is missing a factor of 2.
[27] D. Agassi, H. A. Weidenmüller, and G. Mantzouranis, Phys. Rep., Phys. Lett. **22**, 145 (1975).
[28] E. Lutz and H. A. Weidenmüller, Physica A **267**, 354 (1999).
[29] J. L. Gruver, J. Aliaga, H. A. Cerdeira, P. A. Mello, and A. N. Proto, Phys. Rev. E **55**, 6370 (1998).
[30] O. Bohigas, M.-J. Giannoni, and C. Schmit, Phys. Rev. Lett. **52**, 1 (1984).
[31] M. V. Berry, J. Phys. A **10**, 2083 (1977).
[32] F. Toscano and C. H. Lewenkopf, Phys. Rev. E **65**, 036201 (2002).
[33] I. S. Gradshteyn and I. M. Ryzhik, *Table of Integrals, Series, and Products*, 5th ed. (Academic Press, New York, 1994).
[34] A. Szafer and B. L. Altshuler, Phys. Rev. Lett. **70**, 587 (1993).
[35] B. D. Simons and B. L. Altshuler, Phys. Rev. Lett. **70**, 4063 (1993).
[36] H. De Raedt, Annu. Rev. Comput. Phys. **4**, 107 (1996).
[37] G. Benenti and G. Casati, e-print quant-ph/0112060.